Photoisomerization and Second Harmonic Generation in Disperse Red One-Doped and -Functionalized Poly(methyl methacrylate) Films

R. Loucif-Saïbi, K. Nakatani, and J. A. Delaire*

Laboratoire de Physico-Chimie des Rayonnements (Equipe Cachan de l'U.R.A. 75 C.N.R.S.), Bât. 350, Université de Paris-Sud, 91405 Orsay Cedex, France

M. Dumont and Z. Sekkat

Institut d'Optique Théorique et Appliquée (U.R.A. 14 C.N.R.S.), Bât. 503, Université de Paris-Sud, B.P. 147, 91403 Orsay Cedex, France

Received July 28, 1992. Revised Manuscript Received December 7, 1992

We have demonstrated that photoisomerization of disperse red one (DR1) dissolved in poly(methyl methacrylate) (PMMA) matrix can induce a decrease in second harmonic generation (SHG). This decrease of the SHG signal ($I_{2\omega}$) was measured on electric field-poled thin films of this doped polymer (guest–host system). It has an irreversible component due to irreversible disorientation of the molecules and a reversible one due to cis-trans isomerization without any orientation change of the molecules. Opposite to this case, the decay of $I_{2\omega}$ is mainly irreversible in DR1-functionalized PMMA copolymer system studied under the same conditions. The quantum yields for trans → cis (Φ_{tc}) and cis → trans (Φ_{ct}) photoisomerization have been determined at room temperature for the doped polymer (Φ_{tc} = 0.11 and Φ_{ct} = 0.7), and the absorption spectrum for the thermally unstable cis form has been deduced.

Introduction

In the field of nonlinear optics, one of the great advantages of dye-doped or -functionalized polymers is their ability to form thin films suitable for integrated optics. Another advantage is due to the photochemical properties of the dye or the polymer that can be transformed by visible or UV light, which allows very interesting physical or physicochemical changes of the film. These changes can induce refractive index variations.[1,2] These variations could be used to make low loss channel wave guides.

In a previous paper,[3] we have shown that the reversible photoisomerization of disperse red one (DR1) in poly(methyl methacrylate) (PMMA) thin film induces a reversible refractive index change. In this paper, we demonstrate that, in a polymer film previously poled under an electric field, photoisomerization also induces a change in the second-order susceptibility. The contributions of different mechanisms are brought to evidence by the differences between the behavior of guest–host polymers and copolymers. Furthermore, we have investigated in more detail, from a photochemical point of view, the photoisomerization processes of DR1 in a PMMA matrix.

Experimental Section

Polymer Films. Doped polymer films of DR1 (Aldrich product) in PMMA (Elvacite 2041) were prepared by spin cast techniques on a glass plate from a solution of 4% w/w of PMMA in chloroform added with DR1 (5% w/w relative to PMMA). The films (thickness of around 1 μm) were dried at 120 °C for 2 min and then poled by the Corona technique[4,5] under a voltage of +5 kV applied to a gold-plated stainless steel needle located 1 cm above the surface of the film. The high voltage was applied during 2 min when the temperature of the film was 120 °C and maintained during the cooling of the film down to room temperature.[6]

The PMMA–DR1 copolymer (see Figure 1) was synthesized at L.C.R.-Thomson-C.S.F. The GPC analysis performed by Advanced Materials (I.C.I.) gave M_n = 27 200 and M_w = 82 800 for this polymer. The T_g value, determined by differential scanning calorimetry, was 125 ± 1 °C. The preparation of the copolymer films was slightly different from that for the doped polymer: (i) the copolymer was added with pure PMMA polymer (10% w/w of PMMA-DR1 in PMMA) in order to get the same optical density and thickness as the doped polymer; (ii) after spin casting the chloroform solution, the polymer film was heated at 120 °C for 1 h (instead of 2 min for the doped polymer film).

Second Harmonic Generation (SHG) Measurements. SHG was carried out using, as the probe (or analysis) beam, the fundamental (1.064 μm) of a Q-switched mode-locked picosecond Nd:YAG laser (10 Hz). The experimental setup is shown in Figure 2. The poled film was mounted on a rotating plate moved by a step motor. After integration, the SHG signal ($I_{2\omega}^{f}$) was compared with the integrated SHG signal generated by a sample of urea powder ($I_{2\omega}^{ref}$). The ratio $I_{2\omega}^{f}/I_{2\omega}^{ref}$ was calculated by a Keithley multimeter connected to a computer.

For photoisomerization experiments the visible light of an argon ion laser (488 nm), the pump (or irradiation) beam, was focused on the film in a crossed beam arrangement with the fundamental of the Nd:YAG laser. The polarization of both beams could be changed by interposing a half-wave plate or a Fresnel rotator followed by a Glan-Taylor polarizer in order to keep equal intensities for different polarizations of both beams.

(1) Yongquiang Shi; Steier, W. H.; Yu, L.; Chen, M.; Dalton, L. R. *Appl. Phys. Lett.* **1991**, *58*, 1131.
(2) Beeson, K. W.; Horn, K. A.; McFarland, M.; Yardley, J. T. *Appl. Phys. Lett.* **1991**, *58*, 1955.
(3) Sekkat, Z.; Morichère, D.; Dumont, M.; Loucif-Saïbi, R.; Delaire, J. A. *J. Appl. Phys.* **1991**, *71*, 1543.
(4) Mortazavi, M. A.; Knoesen, A.; Kovel, S. T.; Higgins, B. G.; Dienes, A. *J. Opt. Soc. Am. B.* **1989**, *6*, 733.
(5) Page, R. H.; Jurich, M. C.; Reck, B.; Sen, A.; Turieg, R. J.; Swalen, J. D.; Bjorklund, G. C.; Grant Willson, C. *J. Opt. Soc. Am. B.* **1990**, *7*, 1239.
(6) Singer, K. D.; Sohn, J. E.; Lalama, S. J. *Appl. Phys. Lett.* **1986**, *49*, 248.

0897-4756/93/2805-0229$04.00/0

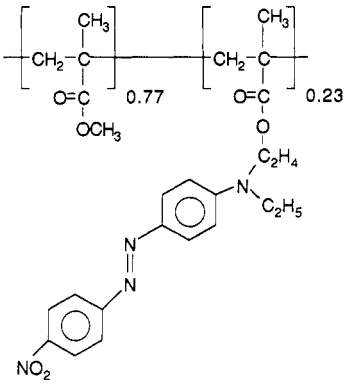

Figure 1. DR1-functionalized PMMA copolymer.

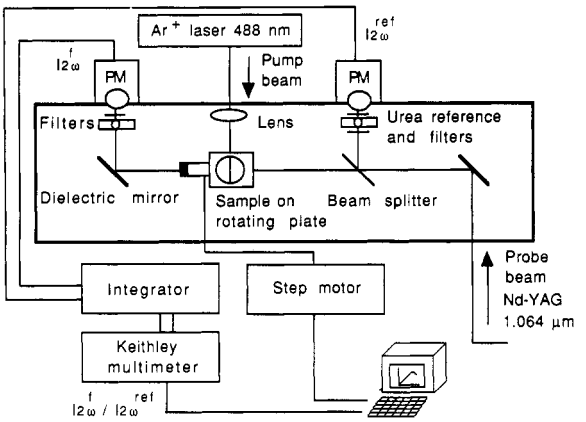

Figure 2. Experimental setup for second harmonic generation measurements.

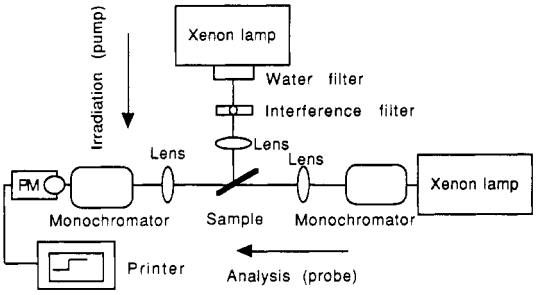

Figure 3. Experimental setup for quantum yield measurements.

Quantum Yield Measurements. Photoisomerization quantum yield determinations were carried out with another experimental setup (see Figure 3) consisting of two perpendicular crossed beams of white light generated by two xenon arcs, focused on the polymer thin film. For the present experiment, the films were not poled. With the arrangement of Figure 3, the pump beam irradiates the film at different wavelengths selected with appropriate interference filters, and the probe beam analyses the temporal change in transmission of the film during and after irradiation. The photon flux of the pump beam was measured with a calibrated radiometer. The flux of the probe beam was strongly attenuated compared to the pump beam.

Results

Reversible Photoisomerization of DR1-Doped and -Functionalized PMMA Polymers. In a previous paper,[3] we have shown that the photoisomerization of *trans*-DR1 in PMMA to the cis form was followed by a fast thermal relaxation:

$$\text{trans} \underset{h\nu,\,\Delta}{\overset{h\nu}{\rightleftarrows}} \text{cis}$$

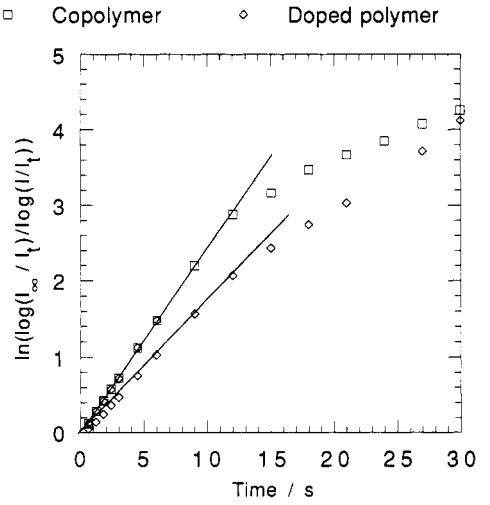

Figure 4. Kinetical study of the thermal cis–trans relaxation. For a first-order kinetics, experimental data should align on a straight line of slope k, the thermal relaxation rate constant. I_∞ and I_t are the transmitted light intensities at the photostationary state and at the trans only state, respectively.

With the experimental setup shown on Figure 3, we followed the photoisomerization of the two polymers by measuring the time dependence of the transmission through the sample. The analysis wavelength was fixed at 490 nm, the maximum absorption wavelength for the trans form of DR1, and the sample was irradiated by the whole xenon lamp spectrum. Both doped and functionalized systems exhibit a totally reversible isomerization. The thermal relaxation of the cis form has been carefully studied. This relaxation (see Figure 4) is not first order, as we already mentioned.[3] Nevertheless, the main component (at least for the first few seconds of the thermal relaxation) is the first exponential one, with a rate constant of 0.18 s^{-1} for the doped system and 0.25 s^{-1} for the functionalized one. For sake of simplicity, we took only this first-order rate constant into account in the following calculations (see eq A1).

Quantum Yield Determination for the DR1-Doped PMMA and Absorption Spectrum of *cis*-DR1 in PMMA. We determined the quantum yields for the photoisomerization from the trans to the cis form (Φ_{tc}), and for the same reaction from the cis to the trans form (Φ_{ct}) in PMMA films at room temperature. We followed the method described by Rau et al.[7] adapted from Fischer's method[8] in the case where the cis isomer is thermally unstable (see Appendix A).

The procedure can be summarized as follows. Since both trans and cis forms can be pumped by the same irradiation and interconverted, we reach an equilibrium of the two isomers called photostationary state. In addition, the thermal cis–trans reaction tends to move this equilibrium in the favor of the trans isomer. Thus, the first part of the experiment consists of determining the absorbance of hypothetical photostationary states of the photoreaction alone by extrapolating the pump beam intensity to infinity for various analysis and irradiation wavelengths. In the second part, these extrapolated values

(7) Rau, H.; Greiner, G.; Gauglitz, G.; Meier, H. *J. Phy. Chem.* **1990**, *94*, 6523.
(8) Fischer, E. *J. Phys. Chem.* **1967**, *71*, 3704.
(9) The extinction coefficient of the trans isomer of DR1 in PMMA film was supposed to be the same as in a chloroform solution of DR1 and PMMA (ϵ_t^{490} = 3.19 × 10^4 L mol^{-1} cm^{-1}).

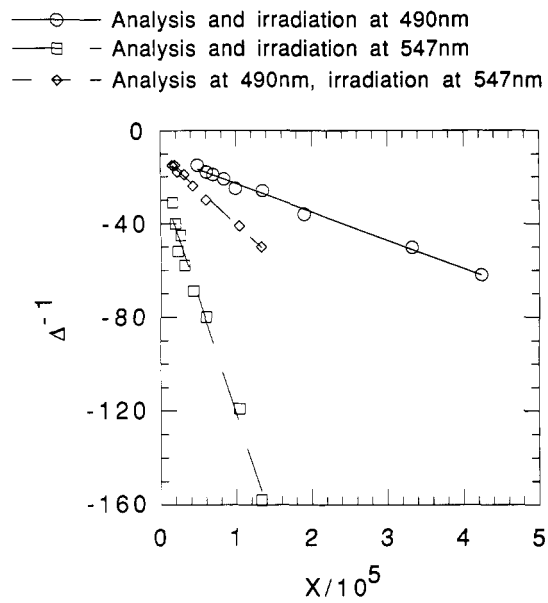

Figure 5. Quantum yield determination of the reversible photoisomerization of DR1 in PMMA film. Note the linear relationship between Δ^{-1} and X (see eq A6).

of the absorbances are treated by Fischer's method to determine the extinction coefficient ϵ_c of the cis form. Finally, the determination of the quantum yields Φ_{tc} and Φ_{ct} from these experimental data is straightforward. We give more experimental details in the next paragraphs.

At least three sets of experiments with the experimental set-up of Figure 3 are required in the method we used. Let us denote by Δ the absorption variation between the trans-only state (A_t) and the photostationary state (A_∞) described above. A set of experiments means measuring the pump beam intensity (I'_0) dependence of Δ^{-1} for a given analysis and irradiation wavelength pair (see eq A6). We chose the three following wavelength pairs (the choice of the wavelengths will be explained later on):

Set no. 1: analysis at 490 nm and irradiation at 490 nm

Set no. 2: analysis at 490 nm and irradiation at 547 nm

Set no. 3: analysis at 547 nm and irradiation at 547 nm

Figure 5 shows the linearity of eq A6. From the intercepts, we reach Δ^∞, the extrapolated value of Δ for infinite intensity. Since A_t can be measured at any wavelength, Δ^∞ values from sets 1 and 3 allow us to determine the ratio Δ^∞ over A_t, namely, δ'^∞ and δ''^∞ (see Appendix A, Fischer's method) for $\lambda' = 490$ nm and $\lambda'' = 547$ nm. Moreover, we get the maximum Δ when analyzing at 490 nm. Let us define ρ as the ratio of Δ^∞ values obtained in sets 1 and 2. According to eq A14, ρ is also the ratio of α'^∞ and α''^∞, the extent of trans → cis conversion for λ' and λ'' irradiation wavelengths at infinite irradiation flux, respectively. The determination of α is then straightforward. In our experimental conditions, the α values were found to be 0.285 and 0.294 at 490 and 547 nm respectively. From these values, and by eq A11, we get the extinction coefficients $\epsilon_c^{490} = 1.63 \times 10^4$ L mol^{-1} cm^{-1} and $\epsilon_c^{547} = 7.0 \times 10^3$ L mol^{-1} cm^{-1}.[9]

Knowing these values, the thermal relaxation rate, and the slopes of the straight lines of Figure 5, a mean value of $\Phi_{tc} = 0.11 \pm 0.03$ was obtained. From the intercepts of these straight lines, we get $\Phi_{ct} = 0.7 \pm 0.1$. Both 490 and

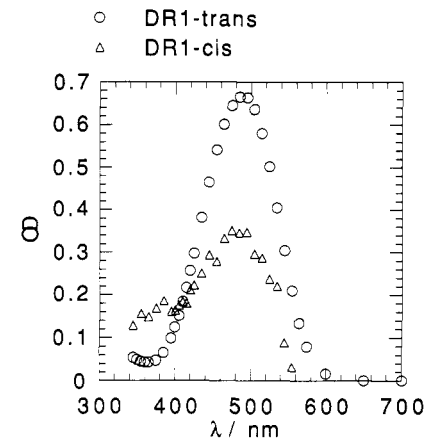

Figure 6. Absorption spectra of *cis*- (determined by Fischer's method) and *trans*-DR1.

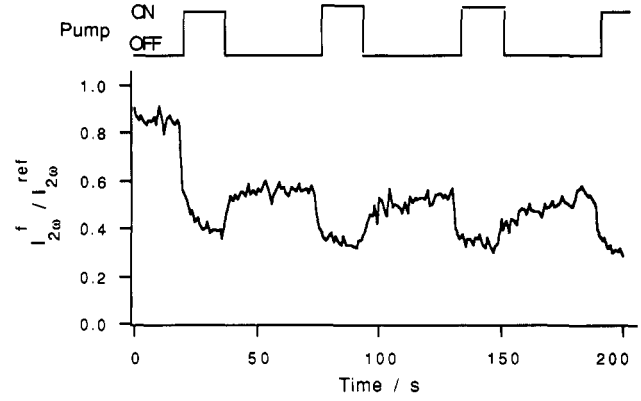

Figure 7. Influence of the photoisomerization on second harmonic generation by a DR1-doped PMMA film (probe and pump beams both S-polarized).

547 nm belong to the same absorption band. Therefore, we considered that the quantum yields do not vary between these two wavelengths.

From the above values of α, it was possible to determine the absorption spectrum of the cis isomer, which is given in Figure 6. An isobestic point was found at 405 nm.

Influence of the Photoisomerization on SHG. We have already shown that photoisomerization of DR1 in PMMA film induces a variation of the refractive index of the solution. We have investigated with the experimental arrangement of Figure 2 the influence of photoisomerization on SHG in both films.

By varying the angle of incidence of the 1.064-μm beam (probe beam) we obtained the usual variation of $I_{2\omega}$, which presents a maximum for the Brewster angle of the interface air-polymer ($i \approx 57°$)[4] for P polarization of the incident beam, and for a lower incidence angle (near 55°) for S polarization. Then we chose a fixed angle of incidence for the probe beam ($i = 30°$), and, in a perpendicular direction, the pump beam (argon ion laser, 488 nm) was focused on the same spot of the polymer film as the probe beam.

Figure 7 shows the change in $I_{2\omega}$ signal of the doped system when both pump and probe beams are S polarized, for a pump beam power of 3 mW cm^{-2}. When the light is on, there is a sharp decay in $\chi^{(2)}$, followed by a slightly slower one. Once the pump beam is off, only a part of the initial $I_{2\omega}$ level is recovered, with a kinetics similar to that of thermal cis–trans photoisomerization. When a second pump cycle is repeated, we then observe a reversible change in $I_{2\omega}$ (see Figure 7). The polarization of both beams has

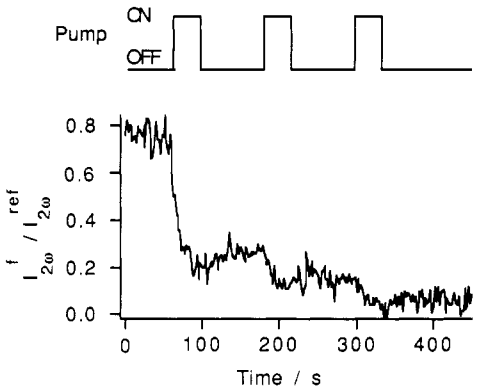

Figure 8. Influence of the photoisomerization on second harmonic generation by a DR1-functionalized PMMA copolymer film (probe and pump beams both S-polarized).

been shown to play a large role: the highest ratio between $I_{2\omega}$ variation and the maximum of the reversible part of $I_{2\omega}$ was observed when both beams were S polarized. Every other thing being equal, this relative decay is 2–2.5 times higher in this polarization configuration than in the case where the probe beam is P-polarized. The decrease in $I_{2\omega}$ was shown to be power dependent: the larger the power, the faster the decrease.

In the case of the copolymer (see Figure 8), the pump beam induces an irreversible power-dependent decay of $I_{2\omega}$ (the higher the intensity of the pump beam, the faster the decay), whatever the polarizations of the beams. As the pump beam is switched off, the drop of $I_{2\omega}$ stops, but resumes when this beam is switched on again. After a total irradiation time of a few minutes, $I_{2\omega}$ falls down to zero.

Discussion

Photoisomerization of DR1-Doped and -Functionalized PMMA Films. We have found that photoisomerization of the push–pull azobenzene derivative DR1 occurs easily in a PMMA film at room temperature. There are many reports in the literature concerning the photochromism of azobenzenes in bulk polymers.[10-12] The free volume of the polymer seems to be an important parameter, all the more as two photoisomerization mechanisms may occur, one from the high energy $\pi \rightarrow \pi^*$ transition, which leads to rotation around the double bond and the other one from the low energy $n \rightarrow \pi^*$ transition which induces isomerization via inversion through one of the nitrogen nuclei.[12] It has been shown that the free volume needed for inversion is lower than that for rotation.

According to Rau's classification,[12] DR1 is a pseudostilbene type azobenzene molecule, which means that the $\pi \rightarrow \pi^*$ transition is overlapping the $n \rightarrow \pi^*$ one, thus giving a large structureless band in the trans isomer, with a strongly solvent dependent polarity maximum. We found that the quantum yields (Φ_{tc} and Φ_{ct}) for DR1 in PMMA are high for long-wavelength irradiation ($\lambda > 400$ nm). Our values can be compared with those obtained in organic glasses at low temperature for 4-nitro-4′-(dimethylamino)azobenzene[13] ($\Phi_{tc} = 0.24$ and $\Phi_{ct} = 0.72$ in a 1:1 methylcyclohexane/toluene mixture at −110 °C). The kinetics of photoisomerization is not first order, contrary to the data obtained for azobenzene in PMMA for 436-nm irradiation wavelength.[14] This complex (at least biexponential) decrease of the absorbance toward the photostationary state might be related to the dual nature of the long-wavelength transition in DR1 (see above).

The thermal cis–trans back-isomerization is fast for both doped and functionalized systems. This is typical of stilbene-like azobenzene molecules.[12] For DR1 in PMMA matrix, the activation energy has been determined and found to be 16 kJ mol^{-1}. This value is matrix- or solvent-dependent. On a similar compound (4-nitro-4′-(dimethylamino)azobenzene), it has been found to be equal to 26 kJ mol^{-1} in toluene solution.[15] The nonmonoexponential thermal back-reaction kinetics also reflects the distribution of the sizes of free sites in PMMA. These phenomena are also probably responsible for the higher thermal back-reaction rate constant for the copolymer.

Photoisomerization and Second Harmonic Generation. When the *trans*-DR1 molecules photoisomerize to the cis form, the molecular hyperpolarizability β decreases. A semiempirical MNDO calculation of β by a finite field method[16,17] gives $\beta° = 44.6 \times 10^{-30}$ esu for the trans form (assumed to have a planar geometry) and $\beta° = 8.4 \times 10^{-30}$ esu for the cis form. The optimal geometry of the cis form was found to be not planar, with both phenyl nuclei twisted relatively to the plane determined by C—N=N—C and making a dihedral angle of 53° with this plane. There is some experimental evidence that such a globular geometry is obtained for the cis compound.[18] Our calculation also shows that the main molecular component of the trans isomer is β_{ZZZ}, Z being the C–N molecular axis. So, with this compound, our hypothesis in Appendix B which stipulates uniaxial molecules is valid. For the cis isomer, β has several components, as a consequence of the globular nature of the molecule.

The observed decrease in $I_{2\omega}$ for the doped system when the pump is on is thus a consequence of the photoisomerization. But, as this process is thermally reversible, it cannot explain the initial irreversible drop of $I_{2\omega}$. Moreover, for the copolymer, $I_{2\omega}$ drops in a totally irreversible way. In the case of the doped polymer, this drop can be explained as follows: a fraction of DR1 molecules among those oriented in large sites, change their orientation as they back-isomerize thermally and photochemically to the trans form after having been photoisomerized to the cis form ("free" molecules). Obviously, this leads to a decrease in the orientational order. The reversible part of $I_{2\omega}$ is due to the fraction of molecules that can only recover their initial orientation ("trapped" molecules). In the copolymer, the DR1 pendent groups seem to have the same behavior as the "free" molecules quoted above. This, of course, can be related to the fact that the first main component of the thermal cis → trans relaxation is higher in the copolymer than in the doped polymer (see Figure 4). This implies that the polymeric chains are flexible and that they do not hinder the movements of the pendent DR1 groups they are covalently linked to. This confor-

(10) Smets, G.; Braeken, J.; Irie, M. *Pure. Appl. Chem.* **1978**, *50*, 845.
(11) Paik, C. S.; Morawetz, H. *Macromolecules* **1976**, *9*, 463.
(12) Rau, H. *Photochemistry and Photophysics*; Rabek, J. F., Ed.; CRC Press: Boca Raton, FL, 1990; Vol. II, p 119 and references therein.
(13) Gabor, G.; Fischer, E. *J. Phys. Chem.* **1971**, *75*, 581.
(14) Shen, Y. Q.; Rau, H. *Makromol. Chem.* **1991**, *192*, 945 and references therein.
(15) Zinsou, A.; Delaire, J. A., unpublished result.
(16) Zyss, J.; Chemla, D. S. *Non-linear Optical Properties of Organic Molecules and Crystals*; Chemla, D. S., Zyss, J., Eds.; Academic Press: Orlando, FL, 1987; Vol. I, p 79 and references therein.
(17) Lalama, S. J.; Garito, A. F. *Phys. Rev. A* **1979**, *20*, 1179.
(18) Uznanski, P.; Krysezewski, M.; Thulstrup, E. W. *Eur. Polym. J.* **1991**, *27*, 41.

mational change of the polymer chain is photoinduced by the photoisomerization reaction and an irreversible change of orientation occurs. In our interpretation of the results, we completely ignored thermal reorientational effects, because we evaluated that the temperature raise of the film under irradiation was too low. We checked this statement by performing the same kind of experiment (influence of irradiation on second harmonic generation) with a PMMA film doped with DANS (4-(dimethylamino)-4′-nitrostilbene), which isomerizes irreversibly with low quantum yield in polymer film, but which absorbs strongly at 457 nm, the argon ion laser line chosen for irradiation. For this polymer, we noticed almost no change of $I_{2\omega}$, in spite of strong absorption by the doped polymer film.

The change in $I_{2\omega}$ with the intensity of the pump beam is very sensitive to the polarization of both pump and probe beams. To understand this sensitivity, we have elaborated the following simplified model. First, we will assume that $I_{2\omega}$ can be calculated for a homogeneous medium with the same hypotheses as in Appendix B. In particular, this implies that Kleinman relationships are obeyed. Obviously, this cannot be true in our experiments as dispersion effects cannot be neglected. Indeed, the second harmonic signal (532 nm) lies close to the absorption maximum of DR1 (488 nm). However, we consider that the following model is a first approach to understand polarization effects. In presence of a polarized pump beam, the distribution function $G(\Omega)$ is perturbed by the excitation. Second, we will assume that the cis compound's orientation is not suitable for absorption and that the photoisomerization can be described by a three-state model (see Appendix C). Furthermore, we will suppose, in order to simplify the calculation, that the cis molecules have a negligible hyperpolarizability ($\beta_{cis} \ll \beta_{trans}$), and finally, we will neglect reorientational effects. These effects do play a role as shown above. The only objective of this model is to account for polarization effects for the reversible change of $I_{2\omega}$.

In the limit of low pump intensity I'_0, the photostationary density of trans molecules is given by (see eq C5):

$$N'(\theta,\varphi) = N(1 - (I'_0/I'_s)\cos^2\theta_p) = N(1 - I\cos^2\theta_p) \quad (1)$$

where N is the initial density of trans molecules and $N'(\theta,\varphi)$ the density of molecules after pumping. The primed quantities refer to those when the irradiation is on. I'_s is the so-called saturation intensity defined in Appendix C. θ_p, the angle between the electric field of the pump beam and the transition dipole moment of the molecule, gets involved in this formula if we take into account the polarization of the pump.

We assume that the transition dipole moment of the molecules has the same direction as the previously defined molecular axis OZ. Pumping breaks the symmetry of the sample and the Kleinman relationships (see Appendix B) are no longer valid. Taking this into account, new calculations similar to those in Appendix B have to be performed.

First of all, the second harmonic polarizations $P'_{NL}{}^S$ and $P'_{NL}{}^P$ for S-probe and P-probe, respectively, have to be rewritten (from eq B3, see Figure 9) as

$$P'^S_{NL} = T^S(\phi)\begin{pmatrix} 0 \\ 0 \\ d_{32} \quad E^2 \end{pmatrix} \quad (2)$$

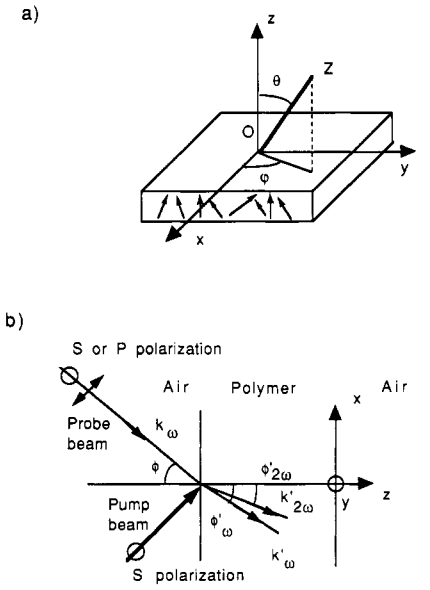

Figure 9. Geometry around the sample for second harmonic generation measurements: (a) Molecular orientation and Euler angles; (b) Beam direction and polarization in the incidence plane.

$$P'^P_{NL} = T^P(\phi)\begin{pmatrix} 2d_{31}E^2 \sin\phi'_\omega \cos\phi'_\omega \\ 0 \\ d_{31}E^2\cos^2\phi'_\omega + d_{33}E^2\sin^2\phi'_\omega \end{pmatrix} \quad (3)$$

where ϕ is the incidence angle of the probe beam, ϕ'_ω the refraction angle of the ω beam inside the sample and E its electric field amplitude. $T^S(\phi)$ and $T^P(\phi)$ are the transmission factors at input air–film boundary for S and P polarizations respectively. d_{31}, d_{32}, and d_{33} are the usual nonlinear coefficients.

Though Kleinman's relationships are no longer valid here, we still have $d_{15} = d_{31}$ (as far as dispersion effects are neglected). Equations B5 and B7 concerning $I_{2\omega}$ are still valid.

Let us focus on the case where the pump polarization is S and develop the calculations of $I'_{2\omega}{}^S$ and $I'_{2\omega}{}^P$. The pump polarization is then parallel to Oy and $\cos\theta_p$ equal to $\sin\theta\sin\varphi$ (θ and φ are the usual Euler angles, see Figure 9). First of all, we have to calculate three non-linear coefficients d'_{31}, d'_{32}, and d'_{33} (instead of two in Appendix B). These coefficients are

$$\begin{aligned} d'_{33} &= {}^1/_2 NF\beta_{ZZZ}\int_0^{2\pi}\int_0^{\pi}\cos^3\theta(1 - \\ &\qquad I\sin^2\theta\sin^2\varphi)G(\theta)\sin\theta\,d\theta\,d\varphi \\ &= {}^1/_2 NF\beta_{ZZZ}[\mathcal{L}_3(u) - {}^1/_2 I\mathcal{L}_3(u) + {}^1/_2 I\mathcal{L}_5(u)] \\ &= d_{33}[1 - {}^1/_2 I + {}^1/_2 I\mathcal{L}_5(u)/\mathcal{L}_3(u)] \end{aligned} \quad (4)$$

d_{33} is the corresponding coefficient when the sample is not irradiated and $\mathcal{L}_n$ is the n-order Langevin function as defined by

$$\mathcal{L}_n(u) = \langle\cos^n\theta\rangle = \frac{\int_0^{2\pi}\int_0^{\pi}\cos^n\theta\exp(-u\cos\theta)\sin\theta\,d\theta\,d\varphi}{\int_0^{2\pi}\int_0^{\pi}\exp(-u\cos\theta)\sin\theta\,d\theta\,d\varphi} \quad (5)$$

where $u = \mu E_p/k_B T$ and where μ is the value of the molecule dipole moment, E_p the intensity of the poling electric field, k_B the Boltzmann constant, and T the temperature.

Similar calculations yield

$$d'_{31} = d_{33}\left[1 - \frac{1}{4}I\frac{\mathcal{L}_1(u) - 2\mathcal{L}_3(u) + \mathcal{L}_5(u)}{\mathcal{L}_1(u) - \mathcal{L}_3(u)}\right]$$

$$d'_{32} = d_{32}\left[1 - \frac{3}{4}I\frac{\mathcal{L}_1(u) - 2\mathcal{L}_3(u) + \mathcal{L}_5(u)}{\mathcal{L}_1(u) - \mathcal{L}_3(u)}\right] \quad (6)$$

In the limit of low polarization ($u \to 0$), these coefficients can be written as follows:

$$d'_{31} = d_{31}[1 - {}^1/_7 I]$$

$$d'_{32} = d_{32}[1 - {}^3/_7 I]$$

$$d'_{33} = d_{33}[1 - {}^1/_7 I] \quad (7)$$

Substitution of these formula in eqs 2 and 3 and then in eqs B5 and B7 yields

$$I'^{S}_{2\omega} = I^{S}_{2\omega}\left(1 - \frac{3I}{7}\right)^2 \approx I^{S}_{2\omega}\left(1 - \frac{6I}{7}\right)$$

$$I'^{P}_{2\omega} = I^{P}_{2\omega}\left(1 - \frac{I}{7}\right)^2 \approx I^{P}_{2\omega}\left(1 - \frac{2I}{7}\right) \quad (8)$$

The unprimed intensities $I_{2\omega}{}^S$ and $I_{2\omega}{}^P$ refer to the second harmonic signal without irradiation.

For low intensity S-polarized pump, the ratio between the relative variations of the second harmonic intensities between the two probe polarizations is equal to 3. This value is to be compared with the experimental data. If we consider exclusively the reversible part of the SHG signal measurement, experimental values spread from 2 to 2.5. The difference may come from the fact that the sample is not very weakly poled (Corona poling technique leads to rather high orientation factor), that the irradiation intensity may not be low enough to allow every approximation we made and that we neglected various parameters of the cis isomer (β_c and ϵ_c).

Conclusion

SHG signal modulation on photochemically active material is a very interesting phenomenon. On one hand, we pointed out this phenomenon and this subject is worth developing toward applications in the field of optical devices. On the other hand, experimental data show that the mechanism is very complex. The orientational effects cannot be dissociated from the photochemical reaction itself. The experimental data of the latter have been compared with a theoretical model we developed above, whereas, for sake of simplicity, we did not take into account the effects of the former. In the present paper, we brought evidence of only the photochemical disorientation of molecules. However, we can take advantage of this effect: we recently found that, instead of inducing disorder, it was possible to make photoassisted poling at room temperature, with a high efficiency in the copolymer system.[19,20] Both phenomena, namely, photoinduced disorientation and photoassisted poling at room temperature, illustrate the wealth of possibilities offered by organic materials.

(19) Sekkat, Z.; Dumont, M. *Appl. Phys. B* **1992**, *54*, 486; *Nonlinear Opt.* **1992**, *2*, 359.
(20) Dumont, M.; Sekkat, Z.; Loucif-Saïbi, R.; Nakatani, K.; Delaire, J. A. *Nonlinear Opt.*, in press.

Acknowledgment. We deeply acknowledge Pierre Le Barny, Philippe Robin, and Evelyne Chastaing of L.C.R.-Thomson-C.S.F. for fruitful discussions and for providing us with samples of the copolymer. We thank Christophe Dhénaut and Jean-François Delouis who efficiently helped us in this study. Finally, we are grateful to Rébéka Andriamanantoa and Stéphane Le Rouzès for activation energy measurements on DR1-doped PMMA films.

Appendix A. Determination of Photoisomerization Quantum Yields in the Case Where the Extinction Coefficient of the Cis Form Is Unknown and the Thermal Relaxation Is Fast

$$\text{trans} \underset{h\nu,\,\Delta}{\overset{h\nu}{\rightleftarrows}} \text{cis}$$

Rau's Method.[7] During irradiation, the concentration c_c of the cis form is given by

$$\frac{dc_c}{dt} = 1000I'_0(1 - 10^{-A'})(\epsilon'_t\Phi'_{tc}c_t - \epsilon'_c\Phi'_{ct}c_c)/A' - kc_c \quad (A1)$$

The primed quantities refer to a measurement at the irradiation wavelength and the unprimed ones to the analysis wavelength.

I'_0 is the incident photon flux, A' the total absorbance of the sample, k the first-order thermal relaxation rate of the cis isomer, ϵ'_t (respectively ϵ'_c) the extinction coefficient of the trans (respectively cis) isomer, Φ'_{tc} (respectively Φ'_{ct}) the quantum yield of the trans → cis (respectively cis → trans) photoisomerization, and c_t (respectively c_c) the concentration of the trans (respectively cis) isomer.

The factor 1000 is required when I'_0 is expressed in mol of photon/cm^2, the extinction coefficients (proportional to the cross section) are in L mol^{-1} cm^{-1} and the concentrations in mol L^{-1}.

Equation A1 can be rewritten as

$$dy/dt = F'(t)\epsilon'_t\Phi'_{tc} - (F'(t)Q' + k)y \quad (A2)$$

if we denote by c_0 the total concentration of DR1 ($c_0 = c_t + c_c$), y the molar fraction of the cis form ($y = c_c/c_0$), $F'(t)$ the following time-dependent function ($F'(t) = 1000I'_0(1 - 10^{-A'})/A'$) and Q' the following factor ($Q' = \epsilon'_t\Phi'_{tc} + \epsilon'_c\Phi'_{ct}$).

For the photostationary state, denoted by index ∞, $dy/dt = 0$, hence

$$\epsilon'_t\Phi'_{tc} = (F'_\infty Q' + k)y_\infty/F'_\infty \quad (A3)$$

The total absorbance $A(t)$ can be expressed as a function of y:

$$A(t) = \epsilon_t c_t L + \epsilon_c c_c L = [(\epsilon_c - \epsilon_t)y + \epsilon_t]c_0 L \quad (A4)$$

In this equation, L is the thickness of the sample along the analysis beam. From eq A3 and A4 written for the photostationary state, we get

$$y_\infty = \frac{F'_\infty\epsilon'_t\Phi'_{tc}}{F'_\infty Q' + k} = \frac{A_\infty - \epsilon_t c_0 L}{(\epsilon_c - \epsilon_t)c_0 L} = \frac{A_\infty - A_t}{(\epsilon_c - \epsilon_t)c_0 L} = \frac{\Delta}{(\epsilon_c - \epsilon_t)c_0 L} \quad (A5)$$

In this equation, both A_∞ and F'_∞ depend on the irradiation intensity I'_0. A_t stands for the optical density of a similar sample containing only the trans isomer. Δ is the optical density's variation when a sample (initially containing only the trans form) is irradiated as far as the photostationary state. The second and the last terms of

this equation can be arranged to give

$$\frac{1}{\Delta} = \frac{F'_\infty Q' + k}{F'_\infty \epsilon'_t \Phi'_{tc} c_0 L(\epsilon_c - \epsilon_t)} = \frac{F'_\infty Q' + k}{F'_\infty A'_t \Phi'_{tc}(\epsilon_c - \epsilon_t)} = \frac{Q'}{(\epsilon_c - \epsilon_t)A'_t \Phi'_{tc}} + \frac{k}{(\epsilon_c - \epsilon_t)A'_t \Phi'_{tc} F'_\infty} = \frac{\epsilon'_t \Phi'_{tc} + \epsilon'_c \Phi'_{ct}}{(\epsilon_c - \epsilon_t)A'_t \Phi'_{tc}} + \frac{k}{1000(\epsilon_c - \epsilon_t)A'_t \Phi'_{tc}} X \quad \text{(A6)}$$

where $X = A'_\infty/(1 - 10^{-A'_\infty})I'_0$.

By plotting the left-hand side of eq A6 versus X at different irradiation intensities I'_0, we may obtain Φ'_{tc} from the slope and Φ'_{ct} from the intercept provided that the extinction coefficients should be known. ϵ_t and ϵ'_t can be experimentally determined,[9] whereas Fischer's method is needed to each ϵ_c and ϵ'_c.

Fischer's Method.[8] This method is valid for systems without thermal relaxation. Therefore, all data concerning the photostationary state were extrapolated to infinite flux. These extrapolated data are denoted by exponent ∞.

Under these conditions, the ratio of the equilibrium concentrations $c^\infty{}_\infty$ are given by

$$\frac{c'^\infty_{t\infty}}{c'^\infty_{c\infty}} = \frac{\Phi'_{ct}\epsilon'_c}{\Phi'_{tc}\epsilon'_t} = \frac{\Phi'_{ct}A'_c}{\Phi'_{tc}A'_t} \quad \text{(A7)}$$

A'_c is the equivalent of A'_t for the cis isomer.

When comparing the results of irradiation at any two wavelengths λ' and λ'', we have two equations of type (A7). By taking the ratio between these two equations, Φ'_{ct}/Φ'_{tc} and Φ''_{ct}/Φ''_{tc} will cancel (assuming that this ratio does not depend on the irradiation wavelength), and we get eq A8:

$$\left(\frac{c'^\infty_{t\infty}}{c'^\infty_{c\infty}}\right)\Big/\left(\frac{c''^\infty_{t\infty}}{c''^\infty_{c\infty}}\right) = \left(\frac{A'_c}{A'_t}\right)\Big/\left(\frac{A''_c}{A''_t}\right) \quad \text{(A8)}$$

If we introduce the extent α^∞ of trans → cis conversion at infinite flux then

$$c^\infty_{t\infty}/c^\infty_{c\infty} = (1 - \alpha^\infty)/\alpha^\infty \quad \text{(A9)}$$

Writing this equation for irradiation wavelengths λ' and λ'' and inserting them in the left-hand side of eq A8 lead to

$$\left(\frac{1 - \alpha'^\infty}{\alpha'_\infty}\right)\Big/\left(\frac{1 - \alpha''^\infty}{\alpha''^\infty}\right) = \left(\frac{A'_c}{A'_t}\right)\Big/\left(\frac{A''_c}{A''_t}\right) \quad \text{(A10)}$$

Now let us express A_c and α in terms of experimental data. The optical density of a mixture of cis and trans, where the overall concentration $c_c + c_t$ is constant (c_0), can always be given by

$$A = A_t(1 - \alpha) + A_c\alpha \quad \text{(A11)}$$

This, of course, is also valid when we consider the infinite flux photostationary state:

$$A_c = A_t + \Delta^\infty/\alpha^\infty \quad \text{(A12)}$$

Recall that Δ has been introduced in eq A5, and it is measured at the same wavelength as the irradiation. The infinite flux extrapolated value Δ^∞ is the intercept of the curve corresponding to eq A6.

Introducing (A12) for λ' and λ'' into (A10), we have

$$\left(\frac{1 - \alpha'^\infty}{\alpha'^\infty}\right)\Big/\left(\frac{1 - \alpha''^\infty}{\alpha''^\infty}\right) = \left(1 + \frac{\Delta'^\infty}{A'_t\alpha'^\infty}\right)\Big/\left(1 + \frac{\Delta''^\infty}{A''_t\alpha''^\infty}\right) = \left(1 + \frac{\delta'^\infty}{\alpha'^\infty}\right)\Big/\left(1 + \frac{\delta''^\infty}{\alpha''^\infty}\right) \quad \text{(A13)}$$

In these equations, δ'^∞ and δ''^∞ denote the relative change of absorbance observed at a wavelengths λ' and λ'' respectively when a solution of *trans*-DR1 is photoequilibrated with an infinite flux light at the respective wavelength.

Furthermore, the ratio ρ ($\rho = \alpha'^\infty/\alpha''^\infty$) of α^∞ at two different excitation wavelengths λ' and λ'' is equal to the ratio of the Δ's measured at the maximum Δ wavelength when irradiating with wavelengths λ' and λ''. We finally get

$$\alpha''^\infty = (\delta'^\infty - \delta''^\infty)/[1 + \delta'^\infty - \rho(1 + \delta''^\infty)] \quad \text{(A14)}$$

All these parameters may be measured experimentally and the numerical value of α''^∞ determined by this equation may then be used to calculate the absorption spectrum of pure cis by means of eq A12. We then get ϵ_c for any wavelength, and its value can be introduced in eq A6, which allows the determination of Φ'_{tc} and Φ'_{ct}.

Appendix B. Calculation of Hyperpolarizability Coefficients and Second Harmonic Intensities for Different Probe Beam Polarizations[4-6,21-24,26]

Let Oz be the normal to the faces of the polymer film, and zOx the incidence plane. Note that Oz is also the poling axis. Let θ be the angle between the molecular axis OZ and Oz (see Figure 9).

The i component P_i of the second-order nonlinear polarization P_{NL} is given by

$$P_i = \sum_{j,k} \chi_{ijk}{}^{(2)} E_j E_k = NF \sum_{j,k} \int (\mathbf{i}\cdot\mathbf{Z})\beta_{ZZZ}(\mathbf{Z}\cdot\mathbf{j})(\mathbf{Z}\cdot\mathbf{k})\, G(\Omega) E_j E_k \, d\Omega \quad \text{(B1)}$$

where $\mathbf{i}$, $\mathbf{j}$, and $\mathbf{k}$ are the unit vectors along the sample axis Oi, Oj, and Ok, $\mathbf{Z}$ is the unit vector along the molecular axis OZ, $\chi_{ijk}{}^{(2)}$ is the quadratic susceptibility, E_j and E_k and the amplitudes of the electric field along axes j and k, respectively, N is the number of dopant molecules per volume unit, F is the product of the local field factors ($F = (f^\omega)^2 f^{2\omega}$), and $G(\Omega)$ is the distribution function according to the solid angle Ω:

$$G(\Omega) = \frac{\exp(-\vec{\mu}\cdot\vec{E}_p/k_B T)}{\int \exp(-\vec{\mu}\cdot\vec{E}_p/k_B T)\, d\Omega} = \frac{\exp(-\vec{\mu}\cdot\vec{E}_p/k_B T)}{\int_0^{2\pi}\int_0^{\pi} \exp(-\vec{\mu}\cdot\vec{E}_p/k_B T)\sin\theta \, d\theta \, d\varphi} \quad \text{(B2)}$$

(21) Eich, M.; Sen, A.; Looser, H.; Bjorklund, G. C.; Swalen, J. D.; Twieg, R.; Yoon, D. Y. *J. Appl. Phys.* **1989**, *66*, 2559.
(22) Eich, M.; Reck, B.; Yoon, D. Y.; Grant Willson, C.; Bjorklund, G. C. *J. Appl. Phys.* **1989**, *66*, 3241.
(23) Wu, J. W. *J. Opt. Soc. Am. B* **1991**, *8*, 142.
(24) Singer, K. D.; Kuzyk, M. G.; Holland, W. R.; Sohn, J. E.; Lalama, S. J.; Comizzoli, R. B.; Katz, H. E.; Schilling, M. L. *Appl. Phys. Lett.* **1988**, *53*, 1800.
(25) Kleinman, D. A. *Phys. Rev.* **1962**, *126*, 1977.
(26) Jerphagnon, J.; Kurtz, S. K. *J. Appl. Phys.* **1970**, *41*, 1667.

where k_B is the Boltzmann constant, T the poling temperature, $\vec{\mu}$ the molecule dipole moment, and $\vec{E}_p$ the poling electric field.

Second Harmonic Intensities as Functions of Nonlinear Coefficients. The symmetry configuration of the poled polymer film is ∞mm. In addition, as far as we consider that dispersion of optical properties are negligible, we have Kleinman's relationships[25] $d_{31} = d_{32}$ and $d_{24} = d_{15}$. Thus, the nonlinear polarization P_{NL} is given by

$$P_{NL} = \begin{pmatrix} 2d_{31}E_xE_z \\ 2d_{31}E_yE_z \\ d_{31}E_x^2 + d_{31}E_y^2 + d_{33}E_z^2 \end{pmatrix} \quad \text{(B3)}$$

with $d_{ij} = {}^1/_2\chi_{ijk}$

Let us consider the two polarizations S (probe beam perpendicular to the incidence plane zOx) and P (probe beam within the incidence plane).

S Polarization. The electric field of the probe beam has only one component $E = E_y$ ($E_x = E_z = 0$). The second harmonic polarization and the corresponding intensity are then given by

$$P_{NL}^S = T^S(\phi)\mathrm{TTT}\begin{pmatrix} 0 \\ 0 \\ d_{31}E^2 \end{pmatrix} \quad \text{(B4)}$$

$$I_{2\omega}^S = \frac{A^S(\phi)|P_{NL}^S|^2}{(n_\omega^2 - n_{2\omega}^2)^2}\sin^2\left(\pi\frac{L}{2L_c}\right) \quad \text{(B5)}$$

L represents the sample thickness, L_c the coherence length, and ϕ the incidence angle of the probe beam, $T^S(\phi)$ and $A^S(\phi)$ are transmission factors that reflect the continuity conditions respectively at input air–film and at output film–air boundaries, and n_ω and $n_{2\omega}$ are the refractive indexes of the sample at the fundamental and the second harmonic frequencies, respectively.

P Polarization. The components of the electric field of the probe beam are $E_x = E\cos\phi'_\omega$, $E_y = 0$ and $E_z = E\sin\phi'_\omega$ (see Figure 9 for ϕ'_ω).

The second harmonic polarization and the corresponding intensity are then given by

$$P_{NL}^P = T^P(\phi)\begin{pmatrix} 2d_{31}E^2\sin\phi'_\omega\cos\phi'_\omega \\ 0 \\ d_{31}E^2\cos^2\phi'_\omega + d_{33}E^2\sin^2\phi'_\omega \end{pmatrix} \quad \text{(B6)}$$

$$I_{2\omega}^P = \frac{A^P(\phi)|P_{NL}^P|^2}{(n_\omega^2 - n_{2\omega}^2)^2}\sin^2\left(\pi\frac{L}{2L_c}\right) \quad \text{(B7)}$$

$T^P(\phi)$ and $A^P(\phi)$ are defined analogously to $T^S(\phi)$ and $A^S(\phi)$.

Nonlinear Coefficients. The nonlinear coefficients d_{ij} can be expressed as functions of β_{ZZZ}.

Application of eq B1 for the symmetry of our sample gives

$$d_{33} = {}^1/_2NF\beta_{ZZZ}\mathcal{L}_3(u) \quad \text{(B8)}$$

By a similar calculation, we get

$$d_{31} = {}^1/_4NF\beta_{ZZZ}(\mathcal{L}_1(u) - \mathcal{L}_3(u)) \quad \text{(B9)}$$

Second Harmonic Intensities in Low Polarization Limit. In the limit of low polarization ($u \to 0$)

$$\mathcal{L}_1(u) \approx u/3 \qquad \mathcal{L}_3(u) \approx u/5 \quad \text{(B10)}$$

$$d_{33} = {}^1/_{10}NF\beta_{ZZZ}u \qquad d_{31} = {}^1/_{30}NF\beta_{ZZZ}u \quad \text{(B11)}$$

The ratio d_{33} over d_{31} is then equal to 3.

By means of eqs (B4)–(B7), the determination of the second harmonic intensities is straightforward.

Appendix C. Simplified Three-Level Model for the Photoisomerization of a Molecule[3]

$$\text{trans} \underset{h\nu,\Delta}{\overset{h\nu}{\rightleftarrows}} \text{cis}$$

In the following, we will consider a three-level model for the photoisomerization of a molecule in an homogeneous medium. We will consider that the extinction coefficient of the cis form is negligible compared with that of the trans form. Although this is not completely true, Figure 6 shows that this assumption is not completely unrealistic. The three-level model is given as

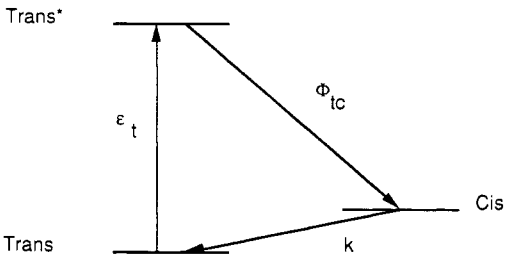

According to this hypothesis, the concentration c_t of the trans form is given by (for definition of the different terms, see Appendix A):

$$dc_t/dt = 1000I'_0(1 - 10^{-A'})\Phi'_{tc} + k(c_0 - c_t) \quad \text{(C1)}$$

If the absorbance is weak ($A' \ll 1$), then this equation simplifies to

$$dc_t/dt = -2300\epsilon'_t\Phi'_{tc}I'_0 + k(c_0 - c_t) \quad \text{(C2)}$$

The integration is then straightforward and gives

$$c_t(t) = \frac{c_0(k + 2300\epsilon'_t\Phi'_{tc}I'_0e^{-t(k+2300\epsilon'_t\Phi'_{tc}I'_0)})}{k + 2300\epsilon'_t\Phi'_{tc}I'_0} \quad \text{(C3)}$$

When the photostationary state is reached, we get the law

$$c_{t_\infty} = \frac{c_0}{1 + (2300\epsilon'_t\Phi'_{tc}I'_0)/k} = \frac{c_0}{1 + I'_0/I'_s} \quad \text{(C4)}$$

with $I'_s = k/2300\epsilon'_t\Phi'_{tc}$.

In the limit of low irradiation fluxes ($I'_0 \ll I_s$), the expression above writes as

$$c_{t_\infty} = c_0\left(1 - \frac{I'_0}{I'_s}\right) = c_0(1 - I) \quad \text{(C5)}$$

where $I = I'_0/I'_s$.